Journal of Geodesy (1999) 73: 568–576

Journal of Geodesy

The modified wave estimator as an alternative to a Kalman filter for real-time GPS/GLONASS–INS integration

J. K. Ray[1], O. S. Salychev[2], M. E. Cannon[1]

[1] Department of Geomatics Engineering, The University of Calgary, 2500 University Drive N.W., Calgary, Alberta, T2N 1N4 Canada
e-mail: cannon@ensu.ucalgary.ca; Tel.: +1 403 220 3593
[2] Department of Inertial Technology, Moscow State Technical University, #5, 2-ya, Baumanskaya, Moscow, 107 005 Russia

Received: 21 April 1998 / Accepted: 5 July 1999

Abstract. The performance of a Kalman filter is essentially limited by the description of the input noise and therefore it is difficult to improve the estimation procedure within the framework of traditional estimation theory. One way to further improve performance is to describe the system in a deterministic sense for a meaningful, but short duration of time. A method called the modified wave estimator (MWE) is used as an alternative to a conventional Kalman filter, where the non-white disturbances are modeled using simple curves or waves, rather than shaping filters driven by known input noise values. The major advantages of this method compared to a conventional Kalman filter are that the estimation accuracy is higher, especially for comparatively weak observables, and is less sensitive to the description of input noise. Results from an integrated global positioning system (GPS)/GLONASS (Global Navigation Satellite System) – inertial navigation system (INS) test are used to demonstrate the performance accuracy of the system using both a Kalman filter and the MWE approach. Results and their analyses are presented with emphasis on situations where improved estimation can be achieved using this new technique.

Key words. Modified wave estimator · Kalman filter · Optimal estimator · GPS/GLONASS–INS · Accuracy

1 Introduction

Kalman filtering has gained widespread use in applied estimation and control due to its desirable characteristics, such as minimization of average mean square errors (MSE), and ease of recursion and implementation (Brown and Hwang 1992). It renders optimal estimation in such cases as a minimum mean square error (MMSE) estimate, a maximum likelihood estimate (MLE), or a maximum a posteriori (MAP) estimate (Gelb 1979; Maybeck 1994). However, it is optimal only if the input and measurement noise values are known accurately and, in addition, the estimation quality is only as good as the underlying model. Furthermore, in a Kalman filter, the weakly observed states require a longer time to converge and thus estimates during this period yield poorer results (Salychev 1995). At steady state the estimation accuracy is limited by the input noise.

Non-conventional approaches proposed by Salychev (1995, 1998), i.e. scalar and wave estimation techniques, are precursors to the algorithm presented below. Scalar estimation is not highly sensitive to the accuracy of the mathematical model and input noise statistics, and allows each of the state variables to be estimated separately. In wave estimation, input disturbances are described by pseudo-deterministic models which are valid over a short time interval. The method described in this paper is related to further developments and enhancements of the wave estimation technique.

Kalman filters have been applied to global positioning system–inertial navigation system GPS–INS integration in many cases over the past decade. The advantages of integrating GPS with INS are discussed by Cox (1980) in terms of improved solution accuracy, aided acquisition and tracking, as well as adaptive tracking. Several authors have described various ways to integrate GPS with INS. For example, Callender (1989) integrated a Ferranti FIN 1041 INS with a P-code receiver using a Kalman filter for airborne applications, while Diesel (1988) described an INS-aided GPS integrity monitoring system. Eissfeller and Spietz (1989) examined the accuracy potential of Honeywell's strapdown laser inertial system to aid kinematic GPS using feed-forward and feedback Kalman filters, while Cannon (1992) achieved accuracies of 5 cm for an integrated road positioning system. Lapucha et al. (1990) developed a highway survey system using a ring-laser gyro INS integrated with a differential carrier-phase GPS

Correspondence to: M.E. Cannon

system, while Wei and Schwarz (1990) devised different decentralized Kalman filter configurations which are flexible to integrate GPS, INS and other sensors. In all cases, Kalman filters of various forms were used. Fundamentals of INS can be found in Britting (1971) on a comprehensive review of GPS and inertial integration is available in Greenspan (1996).

In this paper, the concept of a modified wave estimator (MWE) is presented and compared to a conventional Kalman filter in order to evaluate the accuracy performance of a GPS/GLONASS–INS (Global Navigation Satellite System) system using both estimation techniques.

2 Modified wave estimation

The MWE technique was described by Salychev (1995) and is based on the principle that input disturbances can be described by deterministic means for short time periods. Instead of using a shaping filter driven by white Gaussian noise, the MWE models input disturbances as known base functions with unknown intensities which can be estimated (see Figs. 1 and 2).

A similar technique is described by Lichten (1990) with regard to the GPS inferred positioning system (GIPSY), a multi-satellite batch sequential pseudo-epoch state process noise filter for estimation of GPS satellite orbits and other parameters. In this method, the filter divides the measurements into finite time intervals, known as batches, during which all the process noise parameters are assumed to be piecewise constant. After filtering is complete, a smoother works recursively backwards in time to optimally update the computed estimates and covariances. Another method that is related to MWE is the Schmidt–Kalman filter (Brown and Hwang 1992) wherein only the desired states are estimated, taking into account the influence of other non-estimated states.

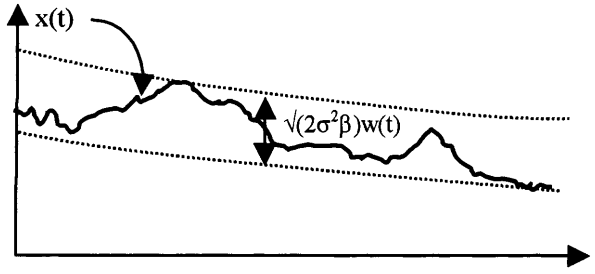

Fig. 1. Shaping filter representation of input disturbances in a conventional Kalman filter

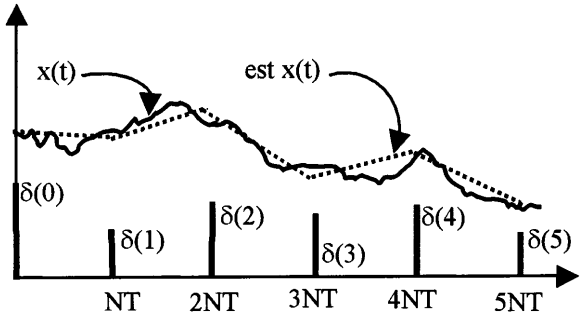

Fig. 2. Wave representation of input disturbances in the modified wave estimator

In MWE, the input disturbance can be represented as follows:

$$w(t) = c_1 f_1(t) + c_2 f_2(t) + \cdots + c_n f_n(t) \tag{1}$$

where $w(t)$ is the input disturbance, $f_1(t) \ldots f_n(t)$ are known base functions, e.g. horizontal lines, inclined lines, exponential functions and $c_1 \ldots c_n$ are unknown coefficients which vary from one instant in time to the next.

The system is represented as

$$x_k = \Phi_{k,k-1} x_{k-1} + \delta_{k-1} \tag{2}$$

and the measurement model assuming a stationary process is given as

$$z_k = H x_k + v_k \tag{3}$$

where

x_k	is the total state vector
$\Phi_{k,k-1}$	state transition matrix
δ_{k-1}	consists of impulse functions appearing once every N time steps. Their intensities are the same as the unknown coefficients of the wave description
z_k	measurement vector
H	observation matrix
v_k	white Gaussian measurement noise with zero mean and known covariance R_k.

Using Eqs. (1)–(3), it is possible to describe the system in a deterministic sense during a short time interval NT, where T is the sampling period and NT is called the cycle time. The main issue is then the selection of an appropriate cycle time. A small cycle time allows a more accurate representation of the system, but it may not be sufficient for all the state vectors to converge. On the other hand, a large cycle time ensures convergence, but may degrade the estimation accuracy. A more prudent approach is to segregate the state variables into two groups based on their degree of observability. The observability condition is defined as the ability to determine the state variables from the given measurements (Gelb 1979). In this approach, the first group is comprised of all the strongly observed states, normally the basic system model, and the second part comprises all the weakly observed states, normally the state variables for wave representation. It is then possible to have a shorter wave cycle ensuring convergence of only the strongly observed states. Weakly observed states, even though not converged during the cycle time, can be estimated separately in a second group.

Through separation, the basic system model has two components in a wave cycle. The first component is the influence of the strongly observed states on themselves and the second component is the influence of the weakly observed states on the strongly observed states. There-

fore, the basic model of the system can be completely described as

$$x_k = x_k^0 + x_k^1 \tag{4a}$$

with initial condition $x_0^0 = x_0$; $x_0^1 = 0$

$$\begin{aligned} x_k^0 &= \Phi_{k,k-1} x_{k-1}^0 \\ x_k^1 &= \Phi_{k,k-1} x_{k-1}^1 + G e_{k-1} \\ e_k &= L_{k,k-1} e_{k-1} \end{aligned} \tag{4b}$$

where

x_k	is the vector of strongly observed states ($n \times 1$)
x_k^0	influence of strongly observed states on themselves ($n \times 1$)
x_k^1	influence of weakly observed states on strongly observed states ($n \times 1$)
$\Phi_{k,k-1}$	state transition matrix of the strongly observed states ($n \times n$)
G	influence matrix expressing the effect the weakly observed states on the strongly observed states ($n \times k$)
e_k	vector of the weakly observed states ($k \times 1$)
$L_{k,k-1}$	state transition matrix of the weakly observed states ($k \times k$).

Often, weakly observed states in vector e_k are the state variables representing wave functions with unknown coefficients.

Following the above, the a posteriori estimate of the first component at the kth epoch in a wave cycle is

$$\hat{x}_k^0 = \Phi_{k,k-1} \hat{x}_{k-1}^0 + K_k (z_k - H \Phi_{k,k-1} \hat{x}_{k-1}^0) \tag{5}$$

and the estimation error is

$$\begin{aligned} \tilde{x}_k^0 &= \hat{x}_k^0 - x_k^0 \\ &= (I - K_k H) \Phi_{k,k-1} \tilde{x}_{k-1}^0 + K_k H D_k e_0 + K_k v_k \\ &= \prod_{i=1}^{k} (I - K_{k+1-i} H) \Phi_{k+1-i,k-i} \tilde{x}_0^0 + \Psi_k e_0 \\ &\quad + \sum_{j=0}^{k-1} \left[\prod_{i=1}^{j} (I - K_{k+1-i} H) \Phi_{k+1-i,k-i} \right] K_{k-j} v_{k-j} \end{aligned} \tag{6}$$

where

$$\begin{aligned} D_k &= \Phi_{k,k-1} D_{k-1} + G L_{k-1,0} \\ \Psi_k &= (I - K_k H) \Phi_{k,k-1} \Psi_{k-1} + K_k H D_k \\ \prod_{i=1}^{j} (I - K_{k+1-i} H) \Phi_{k+1-i,k-i} &= I, \quad \text{if } i > j \end{aligned} \tag{7}$$

In the estimation error, Eq. (6), the first component is due to the error in the initial estimate, the second component is the influence of weakly observed states on strongly observed states, and the third component is due to measurement noise. The matrix D_k propagates the influence of weakly observed states on strongly observed states throughout the wave cycle. This is important because, in conventional Kalman filtering, the convergence of strongly and weakly observed states is sequential (Salychev 1995), with the strongly observed ones converging first. Therefore, the estimation of strongly observed states is affected by weakly observed states, which are yet to converge.

Assuming that the initial estimation error and initial value of the weakly observed states (i.e. $\tilde{x}_0^0$ and e_0) in a wave cycle are uncorrelated, the error covariance is

$$\begin{aligned} P_k &= E[(\tilde{x}_k^0)(\tilde{x}_k^0)^T] \\ &= (I - K_k H) \Phi_{k,k-1} P_{k-1} \Phi_{k,k-1}^T (I - K_k H)^T \\ &\quad + (I - K_k H) \Phi_{k,k-1} \Psi_{k-1} E[e_0 e_0^T] D_k^T H^T K_k^T \\ &\quad + K_k H D_k E[e_0 e_0^T] \Psi_{k-1}^T \Phi_{k,k-1}^T (I - K_k H)^T \\ &\quad + K_k H D_k E[e_0 e_0^T] D_k^T H^T K_k^T + K_k R_k K_k^T \end{aligned} \tag{8}$$

The optimal gain for minimum error covariance is obtained when $(\partial \,\mathrm{trace}[P_k])/(\partial K_k) = 0$. After differentiating P_k and rearranging appropriately, the equation for optimal gain is

$$\begin{aligned} K_k &= \{\Phi_{k,k-1} P_{k-1} \Phi_{k,k-1}^T H^T - \Phi_{k,k-1} \Psi_{k-1} E[e_0 e_0^T] D_k^T H^T\} \\ &\quad \times \{H \Phi_{k,k-1} P_{k-1} \Phi_{k,k-1}^T H^T + H_k D_k E[e_0 e_0^T] D_k^T H^T \\ &\quad + R_k - H \Phi_{k,k-1} \Psi_{k-1} E[e_0 e_0^T] D_k^T H^T \\ &\quad - H D_k E[e_0 e_0^T] \Psi_{k-1}^T \Phi_{k,k-1}^T H^T\}^{-1} \end{aligned} \tag{9}$$

and the corresponding a posteriori covariance matrix is

$$\begin{aligned} P_k &= (I - K_k H) \Phi_{k,k-1} P_{k-1} \Phi_{k,k-1}^T \\ &\quad + K_k H D_k E[e_0 e_0^T] \Psi_{k-1}^T \Phi_{k,k-1}^T \end{aligned} \tag{10}$$

Using Eqs. (5), (9) and (10), it is possible to estimate x_N^0 from the measurement data during the cycle time t_0 to t_N as it is assumed that the strongly observed states converge during this time. This is called forward estimation (see Fig. 3). It is to be emphasized that forward estimation is only used to determine the state vector estimate at the end of the cycle. This estimate is used to reconstruct its value backwards in time to the

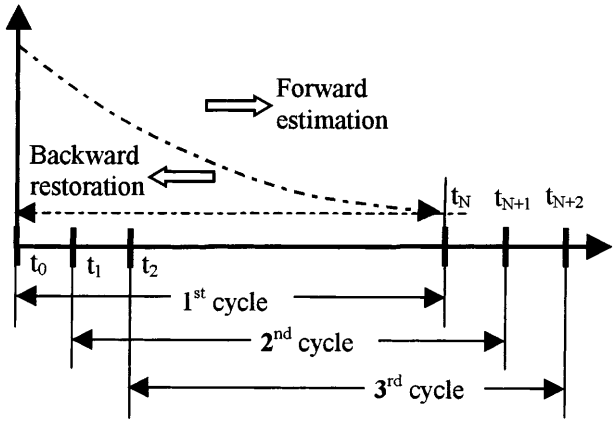

Fig. 3. Modified wave estimator

beginning of the cycle. This is possible due to the piecewise deterministic model description of the system.

In order to reconstruct the estimates at t_1, t_2, t_3 etc. (except at t_0), e_k and x_k^1 need to be estimated. More often than not, however, an estimate of e_k is of no interest, as it normally contains the state variables for wave representation. Therefore, it is advantageous to avoid estimation of e_k, but at the same time account for its influence on the strongly observed states. The following method can be used to achieve this goal.

According to the previous assumptions, at $t = t_0$, $x_0^0 = x_0$. Therefore, if the measurements during the interval t_0 to t_N are used to estimate $\hat{x}_N^0$, it is then possible to reconstruct the initial value $\hat{x}_0^0 = \Phi_{0,N}\hat{x}_N^0 = \hat{x}_0$ without estimating e_k and x_k^1.

Similarly, at the next epoch (t_1), measurements during the interval $t_N + T$ and $t_N + T$ can be used to reconstruct $\hat{x}_1$ as the initial condition for $\hat{x}_0^0$ during that interval (see Fig. 3). In this approach, however, the estimates will have a time lag equal to the wave cycle.

It is also possible to use this technique to do estimation in real time by collecting measurement data for a complete wave cycle (NT, i.e. t_0 to t_N) and then using the previously described algorithm from t_N to t_0 (forward estimation). The initial value at t_N is then reconstructed (backward restoration) in real time. This can be repeated for successive wave cycles, as shown in Fig. 4. In this case, however, no estimate will be available for the duration of the first wave cycle (NT).

3 GPS/GLONASS–INS integration algorithm

GPS/GLONASS and INS have complementary error characteristics; that is, an INS has a good short-term accuracy, but the long-term accuracy is compromised by error growth. In contrast, GPS/GLONASS may be noisier in the short term, but the long term accuracy is consistent. In addition, since GPS/GLONASS relies on line-of-sight from the antenna to the satellite, any shading problems will degrade the accuracy performance. The motivation of GPS/GLONASS and INS integration is to exploit the benefits of each positioning system (Cannon 1992).

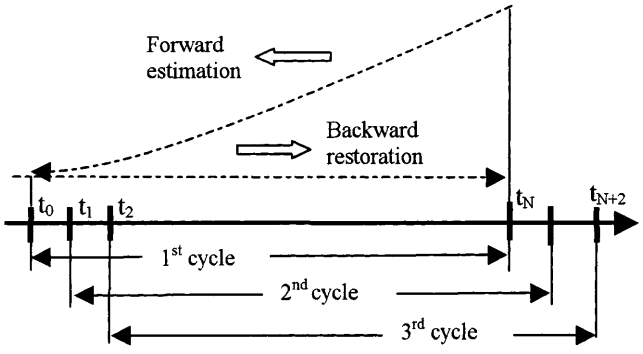

Fig. 4. Real-time modified wave estimator

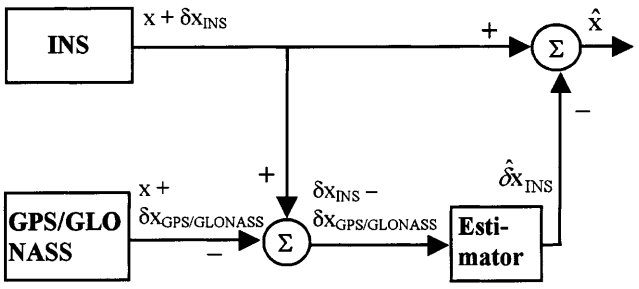

Fig. 5. Open-loop GPS/GLONASS–INS integration scheme

An open-loop GPS/GLONASS–INS integration system can be represented by the simple block diagram shown in Fig. 5 (Maybeck 1994).

In this indirect feed-forward configuration, the estimator plays the crucial role of generating corrections for the INS data. It uses the difference in position and/or velocity between the INS and GPS/GLONASS subsystems to estimate the errors in the inertial system. By subtracting the estimated error from the inertial data, optimal estimates of position, velocity, attitude etc. are determined.

In order to evaluate the performance of the suggested method, the estimator is first implemented by a standard Kalman filter, which is extensively used to integrate GPS–INS systems (Cannon 1992; Schwarz and Zang 1994, Wolf et al. 1997). Secondly, the Kalman filter is replaced by the MWE and their performances are compared in terms of achievable accuracy. Although few tests have been conducted with GPS/GLONASS integrated with an INS, the methodology is essentially the same in this case, since one combined position and velocity is available from the GPS/GLONASS receiver.

3.1 Kalman filter

An INS system for a single axis (e.g. X-axis) may be described as (Maybeck 1994; Salychev 1995)

$$\begin{aligned}
\delta\dot{P}_E &= \delta V_E \\
\delta\dot{V}_E &= -g\phi_N + B_E \\
\dot{\phi}_N &= \frac{\delta V_E}{R} + \delta\omega_N \\
\dot{B}_E &= -\beta_1 B_E + \sqrt{2\sigma_1^2\beta_1}w_1 \\
\delta\dot{\omega}_N &= -\beta_2\delta\omega_N + \sqrt{2\sigma_2^2\beta_2}w_2
\end{aligned} \tag{11a}$$

where

δP_E	is the position error in the X-axis [m]
δV_E	velocity error in the X-axis [m/s]
ϕ_N	attitude error [rad]
B_E	accelerometer bias [m/s^2]
$\delta\omega_N$	gyro drift rate [rad/s]
σ_1, β_1	are the parameters of the shaping filter to represent the accelerometer bias [m/s^2 and s^{-1} respectively]

σ_2, β_2 parameters of the shaping filter to represent the gyro drift rate [rad/s and s^{-1} respectively]
w_1, w_2 driving white noise of unit intensity.

Here, the gyro drift rate and accelerometer bias are modeled by shaping filters using first-order Gauss–Markov processes with different parameters for each. The measurement is the position difference between the INS and GPS/GLONASS, where the latter's position error is assumed to be measurement error.

$$P_{\text{INS}} = P_{\text{True}} + \delta P$$
$$P_{\text{GPS}} = P_{\text{True}} + v$$
$$z_k = P_{\text{INS}} - P_{\text{GPS}} = \delta P + v_k \tag{11b}$$

The process noise matrix for the model is obtained as

$$Q = \int_0^{\Delta T} \Phi(t,\tau) GE[ww^T] G^T \Phi^T(t,\tau) \mathrm{d}\tau$$

$$= \begin{bmatrix} 0 & 0 & 0 & 0 & 0 \\ 0 & S_{p1}\frac{\Delta T^3}{3} & 0 & -S_{p1}\left(0.5\Delta T^2 + \frac{\Delta T^3}{3T_1}\right) & 0 \\ 0 & 0 & S_{p2}\frac{\Delta T^3}{3} & 0 & -S_{p2}\left(0.5\Delta T^2 + \frac{\Delta T^3}{3T_2}\right) \\ 0 & -S_{p1}\left(0.5\Delta T^2 + \frac{\Delta T^3}{3T_1}\right) & 0 & S_{p1}\left(\Delta T + \frac{\Delta T^2}{T_1} + \frac{\Delta T^3}{3T_1^2}\right) & 0 \\ 0 & 0 & -S_{p2}\left(0.5\Delta T^2 + \frac{\Delta T^3}{3T_2}\right) & 0 & S_{p2}\left(\Delta T + \frac{\Delta T^2}{T_2} + \frac{\Delta T^3}{3T_2^2}\right) \end{bmatrix} \tag{11c}$$

where

S_{p1} is the spectral density of the input noise for the accelerometer bias shaping filter [m^2/s^5]
S_{p2} spectral density of the input noise for the gyro drift rate shaping filter [rad^2/s^3]
T_1 time constant of the accelerometer bias Markov process [s]
T_2 time constant of the gyro drift rate Markov process [s]
ΔT sampling interval [s].

Equations (11a)–(11c) form the core model of the Kalman filter for single-axis GPS/GLONASS–INS integration.

3.2 Modified wave estimator

In the MWE, the state variables are segregated into two groups: strongly and weakly observed states. As the difference between the INS and GPS/GLONASS positions is available as a measurement in this case, the position error in the system model is the strongest observable. The velocity error is related to the measurement through first-order differentiation and therefore is a weaker state compared to the position error state. The attitude error is one order weaker compared to the velocity error. Overall these three state variables in the system model are deemed as strongly observed states.

As mentioned earlier, the MWE models the input disturbances, which are often the weakly observed states, using piecewise deterministic curves or waves instead of conventional shaping filters. In this case, the accelerometer bias and gyro drift rate are deemed as weakly observed states and are modeled using wave representation. For example, representing them as inclined lines gives

$$B_E = C_1 + C_2 t \tag{12a}$$

Let $e_1 = B_E$, $e_2 = \dot{B}_E$; then

$$e_1(0) = C_1 = \delta_1; \quad e_2(0) = C_2 = \delta_2 \tag{12b}$$

Similarly, let $e_3 = \delta\omega$, $e_4 = \delta\dot{\omega}$; then

$$e_3(0) = \delta_3; \quad e_4(0) = \delta_4 \tag{12c}$$

Therefore, we have the following formulation:

$$x^0 = [\delta P_E, \delta V_E, \phi_N]^T$$
$$e = [B_E, \dot{B}_E \delta\omega, \delta\dot{\omega}]^T \tag{12d}$$

$$\Phi_{k,k-1} = \begin{bmatrix} 1 & \Delta T & 0 \\ 0 & 1 & -g\Delta T \\ 0 & \frac{\Delta T}{R} & 1 \end{bmatrix} \tag{12e}$$

$$L_{k,k-1} = \begin{bmatrix} 1 & \Delta T & 0 & 0 \\ 0 & 1 & 0 & 0 \\ 0 & 0 & 1 & \Delta T \\ 0 & 0 & 0 & 1 \end{bmatrix} \tag{12f}$$

$$G = \begin{bmatrix} 0 & 0 & 0 & 0 \\ 1 & 0 & 0 & 0 \\ 0 & 0 & 1 & 0 \end{bmatrix} \tag{12g}$$

$$e_0 = [\delta_1, \delta_2, \delta_3, \delta_4]^T \tag{12h}$$

Equations (5), (9) and (10) will be used recursively with various parameters described in Eqs. (12d) through (12h) to estimate the state variables of the strongly observed states.

4 Test description

A GPS/GLONASS–INS system was formed using the Russian strapdown inertial system, I-42, and an Ashtech GG24, which is a combined GPS/GLONASS receiver used to provide independent position information. The GG24 was operated in a mixed mode wherein measure-

ments from GPS and GLONASS satellites were used to determine a single-point position.

The instrumentation was installed in a van and driven at 70–80 km/h through the outskirts of Moscow in a relatively open area with no major obstructions affecting satellite visibility. Approximately 30 min of data was collected using the system on 29 December 1995 with typically 14 satellites in view during the test.

Since GLONASS does not implement selective availability (SA), the nominal horizontal positioning accuracy of the GPS/GLONASS system in a single axis was about 15 m (RMS). Details of GPS/GLONASS experiments and results can be found in Hall et al. (1997).

Differences between INS and GPS/GLONASS positions were used as measurement data input to the estimator, as shown in Fig. 5. A Kalman filter was then used to estimate the position, velocity and attitude errors of the INS.

Truth values were generated by using the same Kalman filter with the difference between the INS and carrier phase *differential* GPS/GLONASS positions as measurement data. In this case, smaller values were used in the R matrix since the differential positions were always better than 0.5 m. Therefore, the position truth trajectory was deemed accurate to the same level. Differences between the Kalman-filter estimated states using the single-point GPS/GLONASS as input, and the truth values using differentially corrected carrier-phase GPS/GLONASS, were used to quantify the estimation error.

A second run of the data was carried out after replacing the Kalman filter by the MWE in the estimator block. Again the estimation errors were obtained as the differences between the MWE estimated values using single-point GPS/GLONASS and truth values of the parameters using differentially corrected carrier-phase GPS/GLONASS.

5 Test results

Figure 6 gives the estimates of the INS position, velocity and attitude errors along a single axis using the Kalman filter, while Fig. 7 gives the corresponding error of these estimates. The error characteristics along the other horizontal axis were similar.

As can be seen, the Schuler oscillation is dominant in the INS position, velocity and attitude error. High-frequency errors, mainly due to GPS/GLONASS measurement errors, are superimposed on the INS errors. A spike between 1000 and 1200 s is observed due to a large error in the single-point GPS/GLONASS measurements.

Estimation errors are the differences between the estimated and truth values, and contain mainly high-frequency components. The position converges quickly, as it has the strongest observability, while attitude converges after position and velocity as it has the weakest observability of the three states. Here, the input noise is $Q = Q_0$, where Q_0 is the average input noise in steady state. Q_0 has been determined by modifying the Kalman filter as an adaptive Kalman filter wherein the measurement noise matrix is kept constant and the input

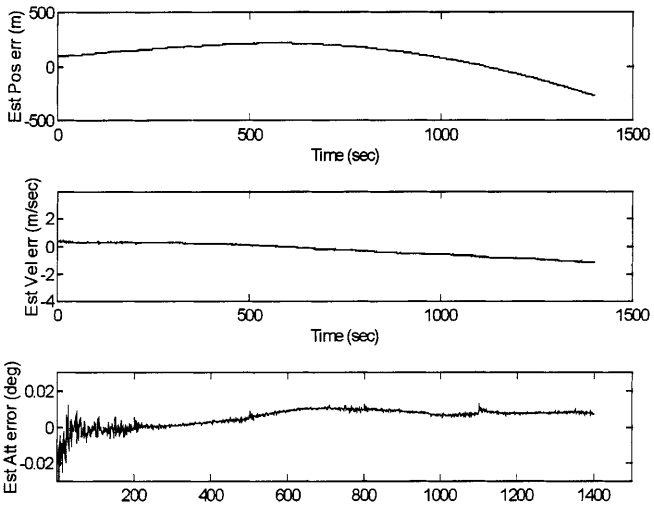

Fig. 6. Estimate of INS position, velocity and attitude errors using INS–single-point GPS/GLONASS derived position in a Kalman filter

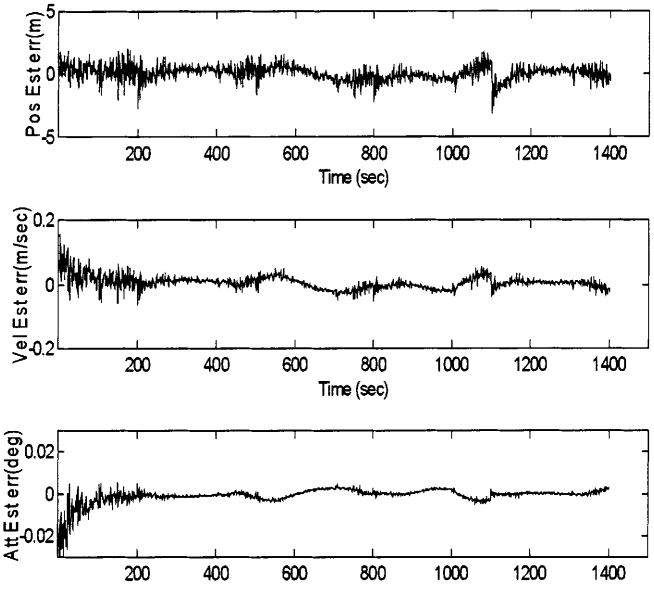

Fig. 7. Estimation error of INS position, velocity and attitude with respect to the INS–dfferential GPS/GLONASS-derived truth values using a Kalman filter

noise is estimated adaptively. The average of the estimated input noise at steady state is computed and used as Q_0 as the system is assumed to be stationary.

Table 1 gives a summary of the estimation accuracy during transition and steady state of the Kalman filter, based on the values shown in Fig. 7. Here, it may be observed that the attitude, being the weakest observable, requires approximately 300 s to reach steady state, wherein statistics of the parameters remain almost unchanged after that time. The mean and root-mean-square (RMS) values of the position, velocity and attitude errors during the transition period depend upon the quality of the initial estimates.

Table 2 gives the revised Kalman filter estimation accuracy with various input noise values derived from

Table 1. Kalman filter estimation accuracy during the transition and steady-state periods using $Q = Q_0$

Transition (s)	Position		Velocity		Attitude	
	Mean (m)	RMS (m)	Mean (m/s)	RMS (m/s)	Mean (deg)	RMS (deg)
100	0.035	0.590	0.005	0.021	−9.3E−4	3.6E−3
200	0.012	0.584	0.003	0.017	−2.8E−4	1.7E−3
250	0.003	0.580	0.002	0.016	−2.0E−4	1.6E−3
300	−0.006	0.558	0.002	0.016	−1.6E−4	1.6E−3
350	0.005	0.550	0.002	0.016	−1.5E−4	1.6E−3

Table 2. Kalman filter estimation accuracy of INS position, velocity and attitude for different input noise values

Input noise	Position		Velocity		Attitude	
	Mean (m)	RMS (m)	Mean (m/s)	RMS (m/s)	Mean (deg)	RMS (deg)
$0.01Q_0$	−0.037	1.408	0.003	0.031	−2.6E−4	1.8E−3
$0.04Q_0$	0.082	1.060	0.004	0.026	−3.1E−4	1.7E−3
Q_0	−0.007	0.558	0.002	0.016	−9.0E−5	1.6E−3
$25Q_0$	−0.058	0.740	0.000	0.023	1.2E−4	2.8E−3
$100Q_0$	−0.061	0.855	−0.001	0.031	1.3E−4	4.0E−3

the average steady-state values. The statistics of this table were generated using only the steady-state values of the errors, i.e. values after the first 300 s. It can be seen that the filter performance is optimum when the input noise is equal to its average steady-state value, as expected. With higher input noise ($>Q_0$) the estimates are noisier, and with lower input noise ($<Q_0$) there is some divergence as the mean error grows. In both situations the RMS errors become larger.

These results illustrate the limitation of a conventional Kalman filter whereby the accuracy is limited by the input noise. Within the scope of this type of model representation, accuracies better than those presented cannot be achieved.

During the implementation of the MWE, all common parameters between the Kalman filter and the MWE were held to the same values. Figure 8 gives the estimation error using the MWE with a wave cycle duration of 300 s, which is the approximate convergence time of the attitude state in the Kalman filter. As a result, no estimate is available for the first 300 s, as mentioned earlier, so that this figure shows the estimation error only after that period.

Table 3 gives a typical case where the variance of e_0 is one tenth of the steady-state input noise. The wave cycle duration is varied widely to determine the estimator performance. Here, it is observed that the estimation accuracy improves with an increasing wave cycle. Estimation accuracies are poorer for wave cycles less than 250 s, but improve substantially for durations of around 350 s.

Table 3 also shows that when the variance of the impulse function is decreased by one order of magnitude compared to the average steady-state input noise, it takes slightly longer for convergence. This is why

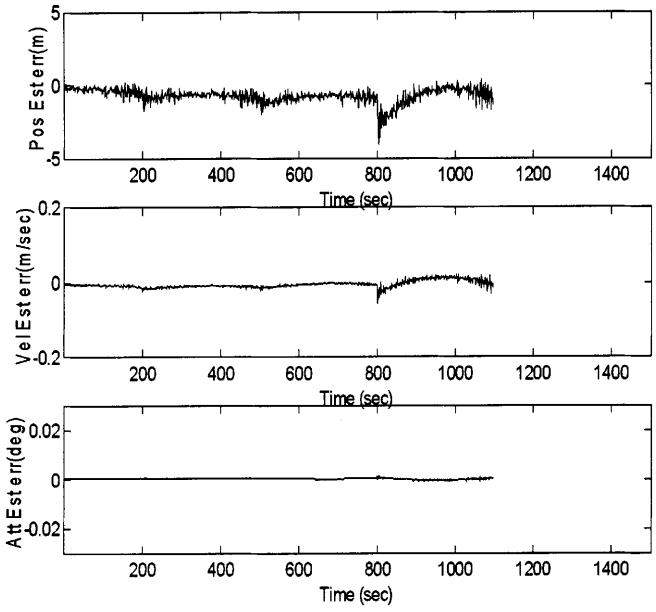

Fig. 8. Estimation error of INS position, velocity and attitude with respect to the INS–differential GPS/GLONASS-derived truth values using the MWE

Table 3. Estimation error of INS position, velocity and attitude using the MWE with $\mathrm{cov}(e_0) = 0.1Q_0$

Wave cycle (s)	Position		Velocity		Attitude	
	Mean (m)	RMS (m)	Mean (m/s)	RMS (m/s)	Mean (deg)	RMS (deg)
150	−0.400	1.247	−0.014	0.032	8.7E−4	2.3E−3
200	−0.258	0.996	−0.008	0.019	3.7E−4	9.7E−4
250	−0.200	0.814	−0.005	0.013	1.9E−4	5.1E−4
300	−0.147	0.695	−0.004	0.009	1.0E−4	2.7E−4
350	−0.128	0.654	−0.003	0.007	−1.0E−5	2.0E−7
400	−0.041	0.512	−0.002	0.007	2.8E−4	4.0E−4

Table 4. Estimation error of INS position, velocity and attitude using the MWE with $\mathrm{cov}(e_0) = 25Q_0$

Wave cycle (s)	Position		Velocity		Attitude	
	Mean (m)	RMS (m)	Mean (m/s)	RMS (m/s)	Mean (deg)	RMS (deg)
150	−0.402	1.249	−0.014	0.034	8.8E−4	2.2E−3
200	−0.258	0.956	−0.006	0.019	−1.8E−4	1.0E−3
250	−0.105	0.748	0.000	0.013	−2.6E−4	9.5E−4
300	−0.018	0.576	0.000	0.013	5.8E−4	1.2E−3
350	−0.002	0.615	0.002	0.014	−6.3E−5	1.3E−3

the estimation accuracy is better with a wave cycle greater than 300 s, the convergence time of the Kalman filter.

Tables 4 and 5 give the estimation accuracies using different values of the variance of e_0. These tables show that the estimation accuracy is inversely related to the variance of e_0, i.e. the lower the variance, the higher the accuracy. With the variance of e_0 much higher compared to the average steady-state input noise (in Table 4), the

Table 5. Estimation error of INS position, velocity and attitude using the MWE with $\text{cov}(e_0) = 0.01Q_0$

Wave cycle (s)	Position		Velocity		Attitude	
	Mean (m)	RMS (m)	Mean (m/s)	RMS (m/s)	Mean (deg)	RMS (deg)
150	−0.400	1.245	−0.014	0.032	8.7E−4	2.3E−3
200	−0.258	0.996	−0.008	0.019	3.7E−4	9.7E−4
250	−0.198	0.814	−0.005	0.013	1.9E−4	5.1E−4
300	−0.135	0.688	−0.003	0.008	1.1E−4	2.7E−4
350	−0.104	0.635	−0.002	0.007	4.9E−5	2.0E−7
400	−0.042	0.611	−0.001	0.006	2.5E−4	1.5E−4

mean of the errors is generally smaller, but the estimates are quite noisy. In contrast, with the variance of e_0 much lower compared to the average steady-state input noise (in Table 5), the estimation errors are substantially reduced. It should also be noted that for higher variance of e_0, a large wave cycle (350 s in Table 4) deteriorates the accuracy as the wave does not appropriately represent the drift and bias errors. This is also evident in particular in the case of attitude in Table 3 for the 400 s wave cycle.

It may be noted that, in contrast to the Kalman filter, lowering the variance has not degraded the performance. This is due to the representation of the input disturbances within a deterministic scope as described earlier and is an advantage of the MWE approach.

Tables 2 (input noise = Q_0), 3 (wave cycle = 350, 400 s) and 5 (wave cycle = 350, 400 s) are used to compare the performance of the Kalman filter and MWE. It is observed that the INS position error estimation accuracy is marginally better with the Kalman filter. However, the velocity error estimation precision is nearly twice as good, and the attitude error estimation precision is nearly eight times better with the MWE. In addition, the improvement is more evident for weakly observed states (i.e. attitude) compared to the strongly observed ones (i.e. position and velocity). This is due to the fact that the attitude error is weakly related to the measurement data and strongly related to the gyro drift rate. As the gyro drift rate is modeled more accurately using wave representation, compared to a shaping filter representation in a conventional Kalman filter, the state variables which are strongly related to this benefit more by wave representation. In contrast, the position error is strongly related to the measurement data and weakly related to the gyro drift rate, hence it is largely affected by the measurement error and benefits least by wave representation.

6 Conclusions

It is observed that the MWE technique renders improved performance in comparison with a Kalman filter in situations where the input disturbances are of low frequency, slowly varying in nature, and are comparatively weak observed states. This approach exploits the fact that even if the system cannot be described in a deterministic form, its forced solution at one point will coincide with the deterministic homogeneous solution. Hence, it is unwise to restrict the estimation accuracy by the level of the input noise if it is possible to reduce the estimation procedure to the homogenous solution reconstruction. This means it is always possible to divide the total estimation time into small pieces and describe each piece using a simple deterministic model. Later, the estimate from each piece may be accumulated for reconstruction of the total state vector behavior. This is why the estimation accuracy has improved in the MWE case.

The accuracy of the MWE technique was compared to that of a standard Kalman filter in an open-loop, indirect feed-forward GPS/GLONASS–INS integrated system. The Russian I-42 strapdown navigation system was used as the INS and an Ashtech GG24 was used as the GPS/GLONASS sensor. Differentially corrected GPS/GLONASS carrier-phase measurements were used to generate the truth trajectory.

Test results show that at steady state the estimate of position error of the INS using a Kalman filter is marginally better than the estimate using an MWE. However, for velocity and attitude, the MWE yields two and eight times better results respectively. The improvement comes from the fact that the disturbances (i.e. the gyro drift rate and accelerometer bias) are represented by a deterministic means rather than by a shaping filter driven by white noise.

Further studies are required to be carried out to investigate the advantages of the MWE for estimation of the weakly observed states (e.g. INS accelerometer bias and gyro drift rate), as it is likely to improve their estimation accuracy even when they have not converged in a conventional Kalman filter.

References

Britting KR (1971) Inertial navigation systems analysis, Wiley-Interscience, New York

Brown RG, Hwang PYC (1992) Introduction to random signals and applied Kalman filtering, 2nd edn, John Wiley, New York

Callender DI (1989) A high performance airborne INS/GPS integrated navigation system, AGARD Lecture Series No. 166, Kalman filter integration of modern guidance and navigation systems. North Atlantic Treaty Organization, pp 4.1–4.15

Cannon ME (1992) Integrated GPS–INS for high-accuracy road positioning, J Surv Eng 118: 103–117

Cox DB (1980) Integration of GPS with inertial navigation systems. Navigation, vol I. The Institute of Navigation, Washington, DC pp 144–153

Diesel JW (1988) GPS/INS integration by functional partitioning. Proc ION GPS-88, Colorado Springs, 19–23 September, pp 301–308

Eissfeller B, Spietz P (1989) Basic filter concepts in the integration of GPS and an inertial ring laser gyro strapdown system. Manuscr Geod 14: 166–182

Gelb A (1979) Applied optimal estimation. MIT Press, Cambridge

Greenspan RL (1996) GPS and inertial integration. In: Global positioning system: theory and applications, Chap 7, vol II, pp 187–220

Hall T, Burke B, Pratt M, Misra P (1997) Comparison of GPS + GLONASS positioning performance. Proc ION GPS-97, Kansas City, Mo, 16–19 September, pp 1543–1550

Lapucha D, Schwarz KP, Cannon ME, Martell H (1990) The use of INS/GPS in a highway survey system. Proc IEEE–PLANS, Las Vegas, NV, 20–23 March, pp 413–420

Lichten SM (1990) Estimation and filtering for high-precision GPS positioning applications. Manuscr Geod, 15: 159–176

Maybeck PS (1994) Stochastic models, estimation, and control, vol 1. Navtech, Arlington, VA

Salychev OS (1995) Inertial surveying: ITC Ltd. experience. Bauman MSTU Press, Moscow

Salychev OS (1998) Inertial systems in navigation and geophysics. Bauman MSTU Press, Moscow

Salychev OS, Bykovsky AV, Arseniev VD, Voronov VV, Lukianov VV, Levtchenkov AV (1994) ITC-2 a Russian generation of inertial survey systems. Int Symp Kinematic Systems in Geodesy, Geomatics and Navigation, Banff, Canada, 30 August–2 September, pp 57–67

Schwarz KP, Li Z, Liu Z (1994) Kalman filtering with fractal noise. Proc Int Symp Kinematic Systems in Geodesy, Geomatics and Navigation, Banff, Canada, 30 August–2 September, pp 155–161

Schwarz KP, Zang G (1994) Development and testing of a low-cost integrated GPS/INS. Proc ION GPS, 7th Int Tech Meeting of the Satellite Division of the Institute of Navigation, Salt Lake City, UT, 20–23 September, pp 1137–1144

Wei M, Schwarz KP (1990) Testing a decentralized filter for GPS/INS integration. Proc IEEE–PLANS, Las Vegas, NV, 20–23 March, pp 429–435

Wolf R, Eissfeller B, Hein GW (1997) A Kalman filter for the integration of a low cost INS and attitude GPS. Int Symp Kinematic Systems in Geodesy, Geomatics and Navigation, Banff, Canada, 3–6 June, pp 143–150